

Study and Simulate Fine Structures Solid State Lasers Using Object Oriented Programming

Author's Details:

- ⁽¹⁾**Bashir Ahmed Malik**-PhD Scholar Department of Physics-Shah Abdul Latif University Khairpur Mirs
⁽²⁾**Pro. Dr. Qurban Ali Bhatti**-Chairman-Department of Physics-Shah Abdul Latif University Khairpur Mirs
⁽³⁾**Dr. Mumtaz Hussain Mahar**-Dean faculty of Sciences-Shah Abdul Latif University Khairpur Mirs

Abstract

This work is based on high resolution laser spectroscopic investigation of La I and La II free atoms. We have employed laser induced fluorescence / Optogalvanic technique using the liquid nitrogen cooled hollow cathode of natural Lanthanum in connection with a frequency stabilized ring dye laser. Laser dyes Coumarin 102 and Coumarin 30 were used as the active medium in the optical blue and green region (4700-5300Å) pumped by multiline ultra-violet (337.5-356.4nm) of Kr-ion and Rhodamine 700 (LD700) pumped by multiline red (647.1-676.4nm) output of Kr-ion laser. These optical regions were explored extensively for the first time in the present work in order to investigate the magnetic dipole coupling constant A and electric quadrupole coupling constant B. For relative frequency reference and linearization of LIF recorded data a temperature stabilized half meter long Fabry-Perot etalon with free spectral range of 149.724MHz for red region and 149.6MHz for blue and green region was used. A commercial Burleigh wave meter was employed with an accuracy of 0.01Å for precise reading of the excitation wavelength. Fourier transform spectra of Lanthanum was also generated in the optical region of 3500 to 8800Å in the graphical form while the data was received in digitalized form by a group in Riga (R. Ferber, A. Jarmola, M. Tamanis, Department of Physics, University of Latvia, Raina Bulvaris, Riga), The same was converted in the graphical form at TU Graz before starting the experimental work. In the FT spectra of La I and La II many Lines were unclassified. In case of La I lines some of the involved levels were also unknown and moreover the hyperfine constants of most of the levels were not known before. In case of La II, the A and B constant of most of the levels in the investigated region were already published via other optical regions. At first main emphasis was given to the measurement of hyperfine constants of already known energy levels and those levels were also investigated which were yet unknown. Through a detailed exploration, more than 155 lines of La I and La II were excited in the aforementioned optical regime of laser dyes during this work. Approximately one half of the lines investigated in this study by means of laser excitation were previously unknown La I lines found on the basis of highly resolved Fourier transform (FT) spectra, having a resolution of 0.03 cm⁻¹. The analysis of spectral lines extracted from already recorded FT spectra using computer programs (Filter and Classification programs) was carried out. Four new levels of La I were discovered and confirmed by the second laser excitation. We have calculated the A and B constant for 99 levels of La I and 28 levels of La II in this work. The data were compared with the already published results of the investigated levels but in different optical regime and found in good agreement within allowed experimental errors. In some cases we observed significant differences in the cited A and B values and our investigated values.

Introduction:

Historically, the search for lasers began as an extension of stimulated amplification techniques employed in the microwave region. Masers, coined from Microwave Amplification by Stimulated Emission of Radiation, served as sensitive preamplifiers in microwave receivers. In 1954 the first maser was built by C. Townes and utilized the inversion population between two molecular levels of ammonia to amplify radiation at a wavelength around 1.25 cm. In 1955 an optical excitation scheme for masers was simultaneously proposed by N. Bloembergen, A.M. Prokhorov, and N.G. Basov. A few years later,

masers were mostly built using optically pumped ruby crystals. In 1958 A. Schawlow and C. Townes proposed extending the maser principle to optical frequencies and the use of a Fabry–Perot resonator for feedback. However, they did not find a suitable material or the means of exciting it to the required degree of population inversion.

Solid Laser Applications

- Solid-state lasers provide the most versatile radiation source in terms of output characteristics when compared to other laser systems. A large range of output parameters, such as average and peak power, pulse width, pulse repetition rate, and wavelength, can be obtained with these systems.
- Today we find solid-state lasers in industry as tools in many manufacturing processes, in hospitals and in doctors' offices as radiation sources for therapeutic, aesthetic, and surgical procedures, in research facilities as part of the diagnostic instrumentation, and in military systems as rangefinders, target designators, and infrared countermeasure systems. The flexibility of solid-state lasers stems from the fact that:
 - The size and shape of the active material can be chosen to achieve a particular performance.
 - Different active materials can be selected with different gain, energy storage, and wavelength properties.
 - The output energy can be increased by adding amplifiers.
 - A large number of passive and active components are available to shape the spectral, temporal, and spatial profile of the output beam With ever-increasing demands on bandwidth, speed and deployment, efforts to reduce the size and cost of communications systems have never been so important.

One technology that has continued to keep pace with demand so far is the [semiconductor laser](#), but can it continue to evolve to provide optical communications systems with higher speed, lower production costs, lower power dissipation and a smaller form factor? Opinions are mixed.

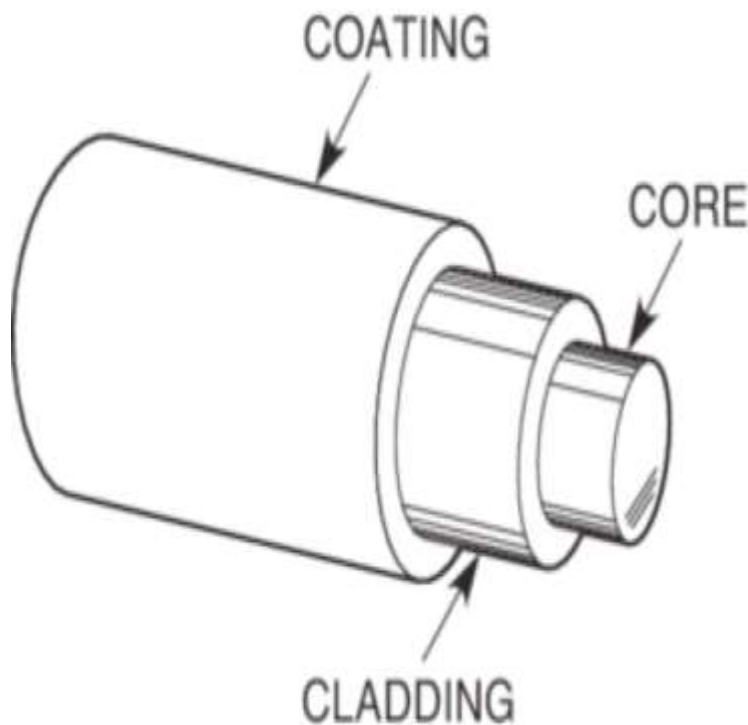
“In optical systems, the laser itself cannot be shrunk; its size is dictated by physics,” said Martin Zirngibl, head of Physical Technologies Research at Bell Labs in Murray Hill, N.J. “However, you can more tightly integrate everything that is needed to operate the laser.”

Optical systems contain footprint-consuming packaging that includes electrical, optical and optoelectronic components, all of which must work together.

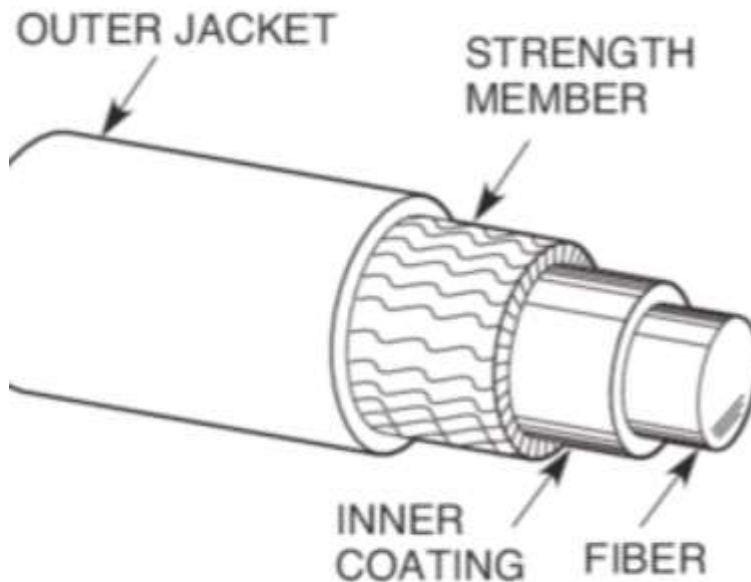
- LASER material is base of Optical Communication. About a half century ago material study and search has been done largely through simulation and its impact in optical communication. In past simulation was done through procedural languages which were very slow for example: interactive data was collected through PASCAL which was then fast over to FORTRAN language to solve Taki-Taupin equation and the data collected was passed over to GOST programming to generate statistically data through graphs. This data provided fabrication of LASERS which requires optical frequency for communication. This was the long procedure and time consuming techniques.
- Through our M.Phil research we have proposed new model which can be implemented with object oriented programming which is only plat form independent but provide unification of implementation with one programme language that is data collection computation of Taki-Taupin equation and statistical data presentation could be done at one work place and can be transferred to any computer machine. So, this will produce more effectiveness for scientist, engineers and technician at same time through internet. So, this will be time saving and cast effective solution for industries producing optical fiber.
- Fiber Optic Basics

Optical fibers are circular dielectric wave-guides that can transport optical energy and information. They have a central core surrounded by a concentric cladding with slightly lower (by $\approx 1\%$) refractive index. Optical fibers are typically made of silica with index-modifying dopants such as GeO_2 . A protective coating of one or two layers of cushioning material (such as acrylate) is used to reduce cross talk between adjacent fibers and the loss-increasing microbending that occurs when fibers are pressed against rough surfaces. For greater environmental protection, fibers are commonly incorporated into cables. Typical cables have a polyethylene sheath that encases the fiber within a strength member such as steel or Kevlar strands.

OPTICAL FIBER



SINGLE FIBER CABLE



- **Problem Statement**

Nowadays, most of the researchers spare their valuable time in the field of Networking and Communication Technologies. Because, the information can be access easily through these both technologies. Almost all networks use fiber optics by using the fine structure solid state laser approach. It has been practically observed that many simulators are available in the market for various networking and communication applications. These simulators were developed with the structured or procedural programming languages i.e. Pascal, Cobol and C. Due to the current advancement in the technology, operating systems and programming languages. These developed simulators are not able to run or execute on the current computers. Hence, it is a great need to convert all the simulators developed in procedural and structural languages into the Object-Oriented languages such as C++ and Java for obtaining the more accurate and efficient results from the available simulators.

Literature Review

- Luccioni et al. [2] analyzed the effect of the detonation of 400 kg TNT in an actual building, the AMIA (Israel's mutual society of Argentina) that suffered a terrorist attack in 1994. They used a hydro-code called AUTODYN [3] to study the complete process numerically from detonation of the explosive charge, to the complete demolition of the building. AUTODYN is capable of interfacing between Eulerian and Lagrangian reference frames and hence can solve coupled fluid-structure interactions. It makes many simplifying assumptions about the structure and the fluid to allow complex simulations in a feasible time. In their simulation (Ref. [2]), they modeled the complete building with reinforced concrete structure and masonry walls The amount of explosive was estimated based on earlier studies. The initial blast wave propagation was simulated in one dimension assuming spherical spreading of the wave until it hit the walls. This solution was then mapped to the 3-D building model and a coupled fluid-structure4 dynamics simulation was carried out. The runtime for the simulation was approximately 310 hrs on a

Pentium IV processor. Reference [2] also compared their results with pictures of the demolished buildings and observed a good qualitative agreement. They concluded that the collapse was due to the gravitational force, initiated by the destruction of the lower columns.

- Mazor et al. [4] theoretically and experimentally investigated the phenomenon of ahead-on collision between a normal shock wave and a rubber-supported plate. They developed a physical model to describe the collision process. The model was based on conservation equations, for both gas and rubber, written in a Lagrangian frame of reference, and on an appropriate stress-strain relation. Three different modes of loading of the rubber were studied: (a) uni-axial stress loading, (b) bi-axial stress loading, and (c) uni-axial strain loading. Numerical solutions of the model were obtained for each of the above-mentioned loading modes. Experiments were conducted in the shocktube facility of the Ernst Mach Institute, Freiburg, Germany. Experiments were conducted to study the rubber response to its collision with normal shock wave for the case of bi-axial stress loading. Reference [4] observed good agreement between the experimental and numerical results for the bi-axial stress loading. Bleakney et al. [5] experimentally investigated the loading on structures due to the impact from a shock wave. They argued that although the pressure falls steadily behind the shock front, the rate of decay is so slow that the first few hundred feet of the wave can be considered flat topped [6].
- Hence, the initial loading on the structures may be studied using shocktube experiments (c.f., Ref. [5]). They conducted a variety of shocktube experiments to provide a large amount of basic data on blast-loading for future analyses by others. However, the results in Ref. [5] are contour plots and it is difficult to obtain quantitative data from the article. Igra and co-workers [7] investigated the efficiency of a double-bend duct in attenuating a blast/shock wave. The article provided a comprehensive experimental and numerical study of shock wave propagation in several different double-bend ducts (Z-shaped tunnel) shown schematically in Fig. 1.1. Such geometries are frequently used in underground shelters, with the aim of attenuating an explosion-generated blast wave before it enters the shelter interior. The experiments were conducted in the 102 mm \AA ~ 178 mm hypersonic shocktube of the Shock Wave Research Center, Institute of Fluid Science, Tohoku University, Japan, and in the 4 cm \AA ~ 11 cm shock tube of the Ernst Mach Institute, Freiburg, Germany. The experimental study included optical diagnostics (interferogram, schlieren and shadowgraph techniques) and pressure measurements. For Reichenbach et al. [8] experimentally and numerically investigated the interaction of a planar shock wave with a square cavity. The experiments were carried out in the shocktube of the Ernst Mach Institute, Freiburg, Germany. This shocktube is designed for using ‘two-dimensional’ models. They used shadowgraph photography to capture the interaction of the shock wave with the cavity explosion-generated blast wave before it enters the shelter interior. The experiments were conducted in the 102 mm \AA ~ 178 mm hypersonic shocktube of the Shock Wave Research Center, Institute of Fluid Science, Tohoku University, Japan, and in the 4 cm \AA ~ 11 cm shock tube of the Ernst Mach Institute, Freiburg, Germany. The experimental study included optical diagnostics (interferogram, schlieren and shadowgraph techniques) and pressure measurements. For Reichenbach et al. [8] experimentally and numerically investigated the interaction of a planar shock wave with a square cavity. The experiments were carried out in the shocktube of the Ernst Mach Institute, Freiburg, Germany. This shocktube is designed for using ‘two-dimensional’ models. They used shadowgraph photography to capture the interaction of the shock wave with the cavity. They also measured the pressure loading at the center of the walls of the cavity for different incident Mach numbers of the shock wave. For the numerical simulations, they used a two-dimensional, second order accurate, finite difference GRP scheme. Their numerical results match their experimental findings both qualitatively and quantitatively. Neuwald, Klein and Reichenbach [9] used a shocktube to study the flow in a chamber subjected to a shock impinging on the entrance to the room. Their interest was in the complex flow field and visualization techniques to analyze the flow field. However, they reported the pressure histories measured at a few points on the walls of the room. They supplemented their experimental observations by their numerical

results obtained using an inviscid Euler code. A more realistic, but involved problem of indoor detonations in buildings was investigated experimentally by Reichenbach and Neuwald [10]. They detonated Nitropenta charges of 0.5 gm in small scale models of a multi-chamber building to obtain a database of pressure loading for indoor detonations. They also examined the influence of the charge position and the effects of venting holes in the detonation chamber. In a two-part paper [11] and [12], Pack investigated the phenomena of reflection and transmission of shock waves from different kinds of boundaries. In Part I [11], Pack showed that for a wave traveling in a barotropic medium (one in which pressure is only a function of density), the nature of the reflected wave is uniquely determined by the relative shock impedances of the medium through which the incident wave passes and the medium upon which it falls. Pack found a simple criterion to determine the nature of reflection of a detonation wave at the end of a block of explosive. He considered specific examples of an explosive in contact with a gas, water or solid surface. In part II [12], Pack examined the motion of an elastic target of finite thickness subject to the impact of a shock wave. The result of the impact is a system of reflected and transmitted waves at the boundaries of the target. Pack [12] examined this process in detail for a one-dimensional system and found formulas for the variation with time of pressure and velocity in the target. Pack assumed for his analysis that the magnitude of the pressure transmitted to the target block remains below the elastic limit of the block. Sir Geoffrey Taylor's publications [13, 14] are perhaps the first published work in the area of blast waves from intense explosions. References [13, 14] are actually two parts of one paper. The first part was written in 1941 during World War II. This paper was the first attempt to describe what mechanical effects could be expected from the explosion of an atomic bomb. The paper was declassified in 1950 and was permitted to be published. Taylor discussed an ideal problem of sudden release of energy in an infinitely concentrated form and calculated the motion and pressure of the surrounding air. He suggested that the explosion results in a spherical shock wave propagating outward whose radius R can be related to the time, energy released, atmospheric density and the ratio of the specific heats. In the second part of the paper [14], Taylor compared his analytical prediction of blast wave propagation to the data collected from some motion picture records of the first atomic explosion in New Mexico. The agreement with the experiments is very good. Igra, Elperin and Ben-Dor [15] numerically investigated the phenomenon of blast wave propagation in dusty gases. The conservation equations for the flow field developed behind a spherical blast wave propagating into a dusty medium (gas seeded with small uniformly distributed particles) were formulated and solved using the random choice method. The random choice method was developed by Glimm [16] and has since been extensively used for solving gas-dynamics problems; see, for example, Miura and Glass [17] and Colella [18]. The main advantage of the random-choice method over other numerical schemes is that it allows high-resolution of shock waves and contact discontinuities, whereas in other finite-difference methods they are smeared over a few mesh points as a consequence of artificial viscosity and truncation error.

Results and Discussions

Application of Fine Structure Solid laser

Due to their high beam quality, fiber lasers are your first choice for precision applications. You can use them to produce narrow weld seams and small cutting kerfs with high quality.

Tru Fiber 500 TruFiber 500 Fiber lasers have been introduced to industrial production for some years now. Their monolithic design allows high beam quality, also known as single mode beam quality. That permits high power density to be generated at the work piece, resulting in high processing speeds for appropriately designed handling systems. Fiber lasers are perfect for scanner welding and always in demand if the application requires particularly narrow weld seams or cutting kerfs.

The Three-Level System

Figure 3.6 shows a diagram that can be used to explain the operation of an optically pumped three-level laser, such as ruby. Initially, all ions of the laser material are in the lowest level 1. Excitation is supplied to the solid by radiation of frequencies that produce absorption into the broad band 3. Thus, the pump

light raises ions from the ground state to the pump band, level 3. In general, the “pump-ing” band, level 3, is actually made up of a number of bands, so that the optical pumping can be accomplished over a broad spectral range. Most of the excited ions are transferred by fast radiationless transitions into the intermediate sharp level 2. In this process the energy lost by the electron is transferred to the lattice.

- Perfect for precision cuts in copper.
- Perfect for precision cuts in bronze.
- The typical application areas of fiber lasers are:
- IT
- Medical device technology
- Precision engineering
- Electrical systems and electronics
- Photovoltaics

Flame cutting

Flame cutting is a standard process primarily used for cutting mild steel. Flame cutting is a standard process that is primarily used for cutting mild steel. In flame cutting, oxygen is used as the cutting gas. The oxygen is blown into the kerf at pressures of up to 6 bar. There, the heated metal reacts with the oxygen: it begins to burn and oxidizes. The chemical reaction releases large amounts of energy – up to five times the laser energy – and assists the laser beam. Flame cutting makes it possible to cut at high speeds and handle jobs involving thick plates such as mild steel with thicknesses in excess of 30 millimeters

Fusion cutting

With fusion cutting you can cut metal as well as other fusible materials, such as ceramics. Different techniques, different results: fast and rough with plasma-assisted fusion cutting (rear) or slow and smooth with conventional fusion cutting (front). Different techniques, different results: fast and rough with plasma-assisted fusion cutting (rear) or slow and smooth with conventional fusion cutting (front).

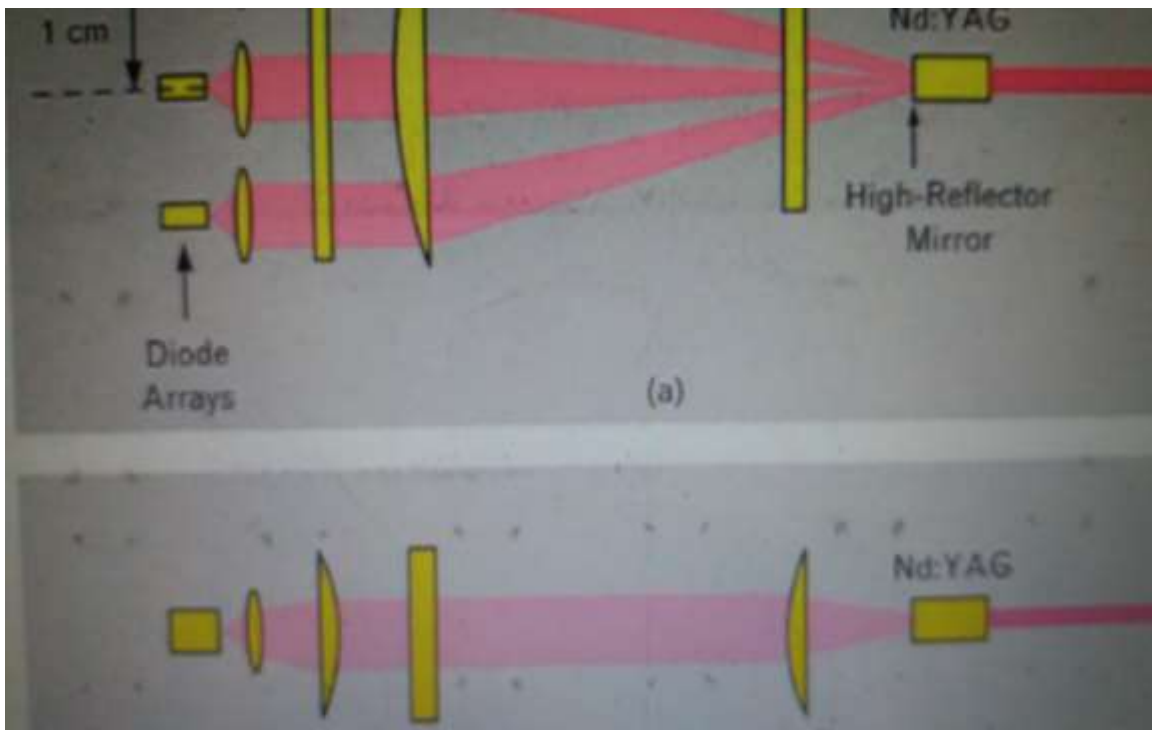
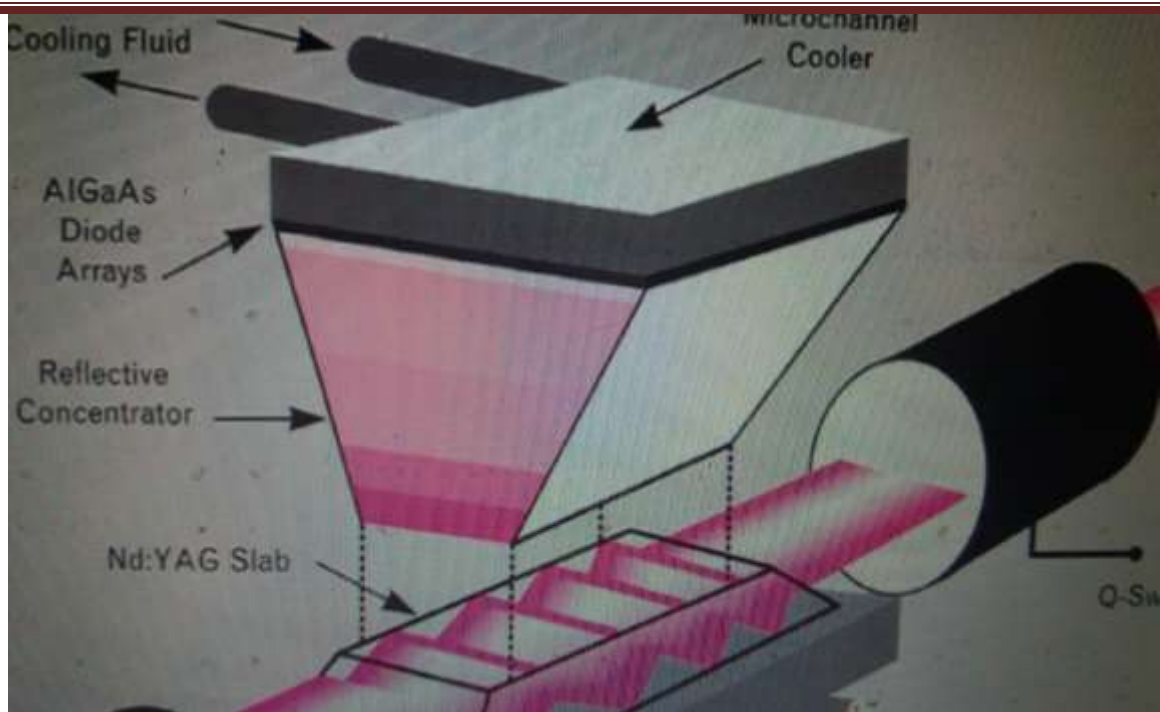
Nitrogen or argon is used as the cutting gas here. The gas is blown through the kerf at pressures ranging from 2 to 20 bar. Argon and nitrogen are inert gases.

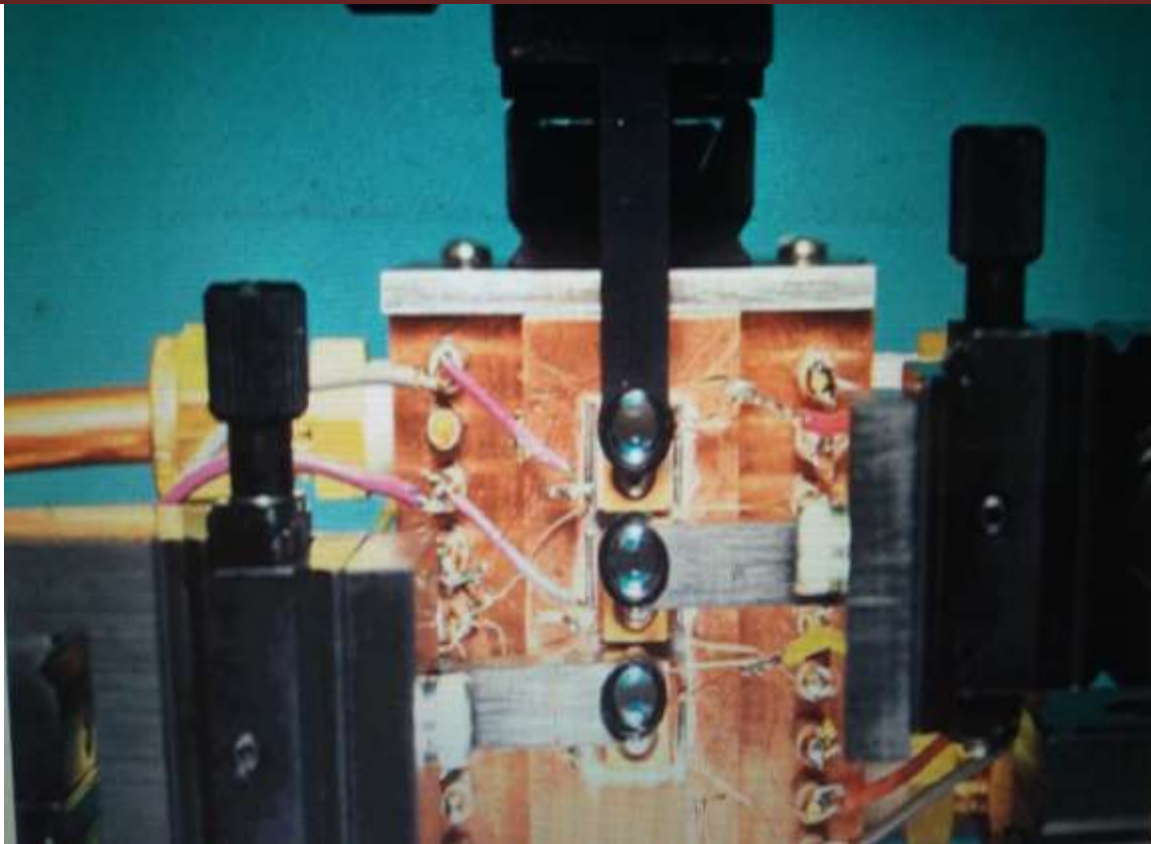
This means that they do not react with the molten metal in the kerf. They simply blow it out toward the bottom. Simultaneously, they shield the cut edge from the air.

The great advantage of fusion cutting: cut edges are oxide free and do not require further treatment. Nevertheless, the laser beam must supply all of the energy needed for cutting. For this reason, cutting speeds as high as those in flame cutting can be achieved only in thin sheets. Piercing is also more difficult. Some cutting systems allow you to use oxygen to pierce the material and then switch over to nitrogen for cutting.

Applications

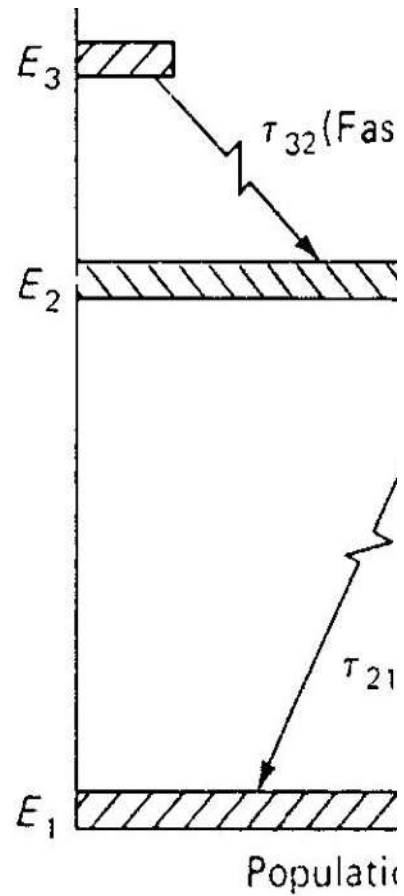
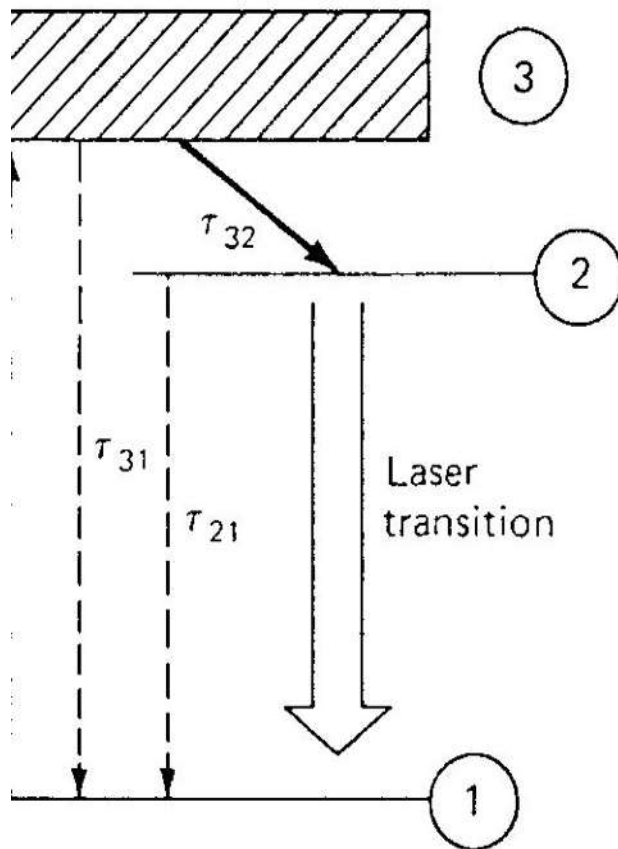
- Solid-State Lasers and Applications covers the most important aspects of the field to provide current, comprehensive coverage of solid-state lasers.
- Because of the favorable characteristics of solid-state lasers, they have become the preferred candidates for a wide range of applications in science and technology, including spectroscopy, atmospheric monitoring, micromachining, and precision metrology. Presenting the most recent developments in the field, Solid-State Lasers and Applications focuses on the design and applications of solid-state laser systems.

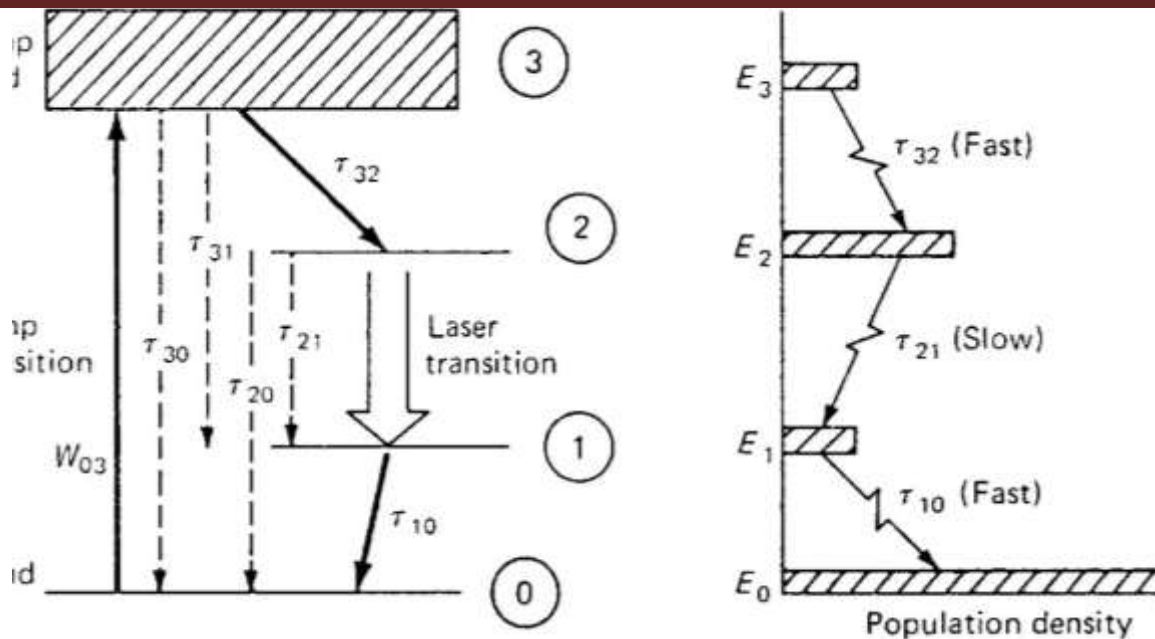




- **The pump beams** are directed out of the plane of the paper. The three black round objects are the
- collimating lenses that are each mounted on translators. The diode laser mount is the gold piece behind
- each collimating lens. dimensional arrays in which the positions of all elements are lithographically
- defined [8]. Monolithic two dimension allenslet arrays have been fabricated at Lincoln
- Laboratory with binary optics techniques [18] and
- mass-transport techniques [19]. The combination of
- monolithic diode arrays and monolithic lenslets reduces
- the number of components in the pump source and
- simplifies the alignment between lenses and large numbers
- of diode lasers. Thermal effects in the gain medium
- Of diode lasers. Thermal effects in the gain medium
- The main disadvantage of diode lasers as pump sources
- is economic; they are much more expensive than
- flashlamps or arc lamps. At current prices, a lamp needed
- to excite a 10-W-average-power laser is a few hundred
- dollars; the cost of an equivalent number of diode lasers

- is tens of thousands of dollars. Projections indicate,
- however, that the price of diode lasers will drop significantly as
- the volume of production increases, in a manner
- similar to other semiconductor technologies such as
- integrated circuits





Properties of Solid-State Laser Materials

Solid-state host materials may be broadly grouped into crystalline solids and glasses. The host must have good optical, mechanical, and thermal properties to withstand the severe operating conditions of practical lasers. Desirable properties include hardness, chemical inertness, absence of internal strain and refractive index variations, resistance to radiation-induced color centers, and ease of fabrication.

Several interactions between the host crystal and the additive ion restrict the number of useful material combinations. These include size disparity, valence, and spectroscopic properties. Ideally, the size and valence of the additive ion should match that of the host ion it replaces.

In selecting a crystal suitable for a laser ion host one must consider the following key criteria:

- The crystal must possess favorable optical properties. Variations in the index of refraction lead to inhomogeneous propagation of light through the crystal which results in poor beam quality.
- The crystal must possess mechanical and thermal properties that will permit high-average-power operation. The most important parameters are thermal conductivity, hardness, and fracture strength.
- The crystal must have lattice sites that can accept the dopant ions and that have local crystal fields of symmetry and strength needed to induce the desired spectroscopic properties. In general, ions placed in a crystal host should have long radiative lifetimes with emission cross sections near 10^{-20} cm^2 .

It must be possible to scale the growth of the impurity-doped crystal, while maintaining high optical quality and high yield

- Oxides

Sapphire. The first laser material to be discovered (ruby laser) employed sapphire as a host. The Al_2O_3 (sapphire) host is hard, with high thermal conductivity, and transition metals can readily be incorporated substitutionally for the Al. The Al site is too small for rare earths, and it is not possible to incorporate appreciable concentrations of these impurities into sapphire. Besides ruby which is still used today, Ti-doped sapphire has gained significance as a tunable-laser material. The properties of ruby and Ti-sapphire will be discussed in Sections 2.2 and 2.10

- **Garnets.**

Some of the most useful laser hosts are the synthetic garnets: yttrium aluminum garnet, $\text{Y}_3\text{Al}_5\text{O}_{12}$

(YAG); gadolinium gallium garnet, $Gd_3Ga_5O_{12}$ (GGG), and gadolinium scandium aluminum garnet $Gd_3Sc_2Al_3O_{12}$ (GSGG). These garnets have many properties that are desirable in a laser host material. They are stable, hard, optically isotropic, and have good thermal conductivities, which permits laser operation at high average power levels.

- **Vanadates**

Nd^{3+} -doped yttrium orthovanadate (YVO_4) has shown a relatively low threshold at pulsed operation. However, early studies of this crystal were hampered by severe crystal growth problems, and as a result YVO_4 was discarded as a host. With the emergence of diode pumping, $Nd : YVO_4$ has become an important solid-state laser material (Section 2.6), because it has very attractive features, such as a large stimulated emission cross section and a high absorption of the pump wavelength, and the growth problem has been overcome for the small crystals required with this pump source.

- **Fluorides**

Doping of fluorides with trivalent rare earth ions requires charge compensation which complicates the crystal growth process. The important representative of this crystal family is yttrium fluoride ($YLiF_4$), a uniaxial crystal. $YLiF_4$ is transparent to 150 nm. Therefore, high-current-density xenon flashlamps which emit strongly in the blue and near-ultraviolet can be used as pump sources without damage to the material. The most common dopant of YLF is Nd^{3+} . $Nd : YLF$ offers a reduction in thermal lensing and birefringence combined with improved energy storage relative to $Nd : YAG$. The thermomechanical properties of $Nd : YLF$, however, are not as good as those of $Nd : YAG$. Details of $Nd : YLF$ are discussed in Section 2.5.

Impact of Laser on Fine Structure

- **The fine structures of integrated circuits and semiconductor devices require operation of the laser at the shortest wavelength possible. Also, by matching the wavelength of a laser to the peak absorption of a specific material, the top layer of a multilayer structure can be removed selectively without damage to the layers underneath.**
- **All Nd : glass lasers employed in inertial confinement fusion experiments are operated at the third harmonic, i.e., 352 nm, because the shorter wavelength is more optimum for pellet compression compared to the fundamental output. Medical applications require solid-state lasers operating in a specific spectral range for control of the absorption depth of the radiation in the skin, tissue, or blood vessels. Frequency agility is required from lasers employed in instruments used for absorption measurements, spectroscopy, sensing devices, analytical chemistry, etc. A fixed or tunable laser in conjunction with harmonic generators and/or an optical parametric oscillator is usually employed to meet these requirements.**

TABLE 2.2. Physical and optical properties of Nd : YAG.

Chemical formula	Nd : Y ₃ Al ₅ O ₁₂
Weight % Nd	0.725
Atomic % Nd	1.0
Nd atoms/cm ³	1.38 × 10 ²⁰
Melting point	1970 °C
Knoop hardness	1215
Density	4.56 g/cm ³
Rupture stress	1.3–2.6 × 10 ⁸ kg/cm ²
Modulus of elasticity	3 × 10 ¹¹ kg/cm ²
Thermal expansion coefficient	
[100] orientation	8.2 × 10 ⁻⁶ °C ⁻¹ , 0–250 °C
[110] orientation	7.7 × 10 ⁻⁶ °C ⁻¹ , 10–250 °C
[111] orientation	7.8 × 10 ⁻⁶ °C ⁻¹ , 0–250 °C
Linewidth	120 GHz
Stimulated emission cross section	
R ₂ - Y ₃	σ = 6.5 × 10 ⁻¹⁹ cm ²
⁴ F _{3/2} - ⁴ I _{11/2}	σ = 2.8 × 10 ⁻¹⁷ cm ²
Fluorescence lifetime	230 μs
Photon energy at 1.06 μm	hν = 1.86 × 10 ⁻¹⁷ J
Index of refraction	1.82 (at 1.0 μm)

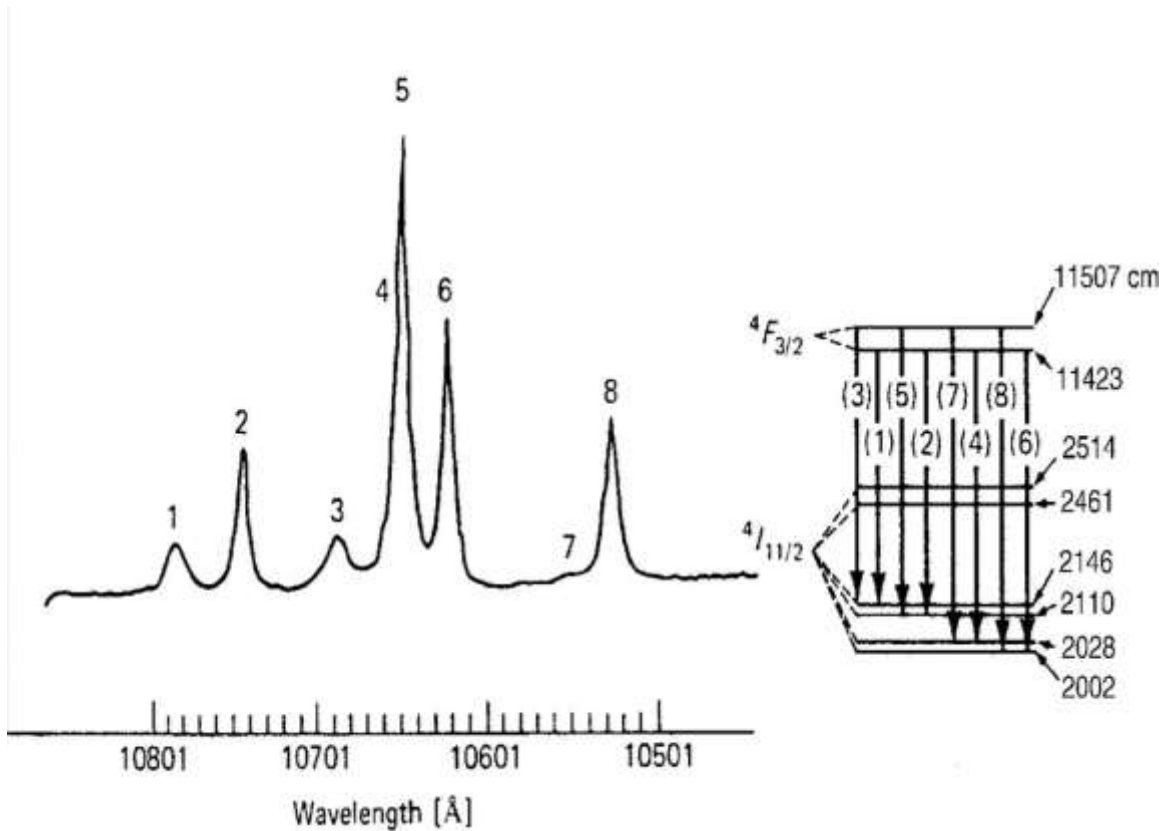


TABLE 2.4. Physical and optical properties of Nd-doped glasses.

Glass Type	Q-246 Silicate (Kigre)	Q-88 Phosphate (Kigre)	LHG-5 Phosphate (Hoya)	LHG-8 Phosphate (Hoya)	LG-670 Silicate (Schott)	LG-760 Phosphate (Schott)
Peak wavelength [nm]	1062	1054	1054	1054	1061	1054
Cross section [$\times 10^{-20}$ cm ²]	2.9	4.0	4.1	4.2	2.7	4.3
Fluorescence lifetime [μ s]	340	330	290	315	330	330
Linewidth FWHM [nm]	27.7	21.9	18.6	20.1	27.8	19.5
Density [gm/cm ³]	2.55	2.71	2.68	2.83	2.54	2.60
Index of refraction [Nd]	1.568	1.545	1.539	1.528	1.561	1.503
Nonlinear coefficient [10^{-16} cm ³ /W]	3.74	2.98	3.48	3.10	3.78	2.90
dn/dt (20–40 °C) [10^{-5} / °C]	2.9	-0.5	8.6	-5.3	2.9	-6.8
Thermal coefficient of optical path (20–40 °C) [10^{-5} / °C]	+8.0	+2.7	+4.6	+0.6	8.0	—
Transformation point [°C]	518	367	455	485	468	—
Thermal expansion coefficient (20–40 °C) [10^{-5} / °C]	90	104	86	127	92.6	138
Thermal conductivity [W/m °C]	1.30	0.84	1.19	—	1.35	0.67
Specific heat [J/g °C]	0.93	0.81	0.71	0.75	0.92	0.57
Knoop hardness	600	418	497	321	497	—
Young's modulus [kg/mm ²]	8570	7123	6910	5109	6249	—
Poisson's ratio	0.24	0.24	0.237	0.258	0.24	0.27

Impact of Object Oriented Programming on Equation based Modeling

section $\sigma(\nu)$,

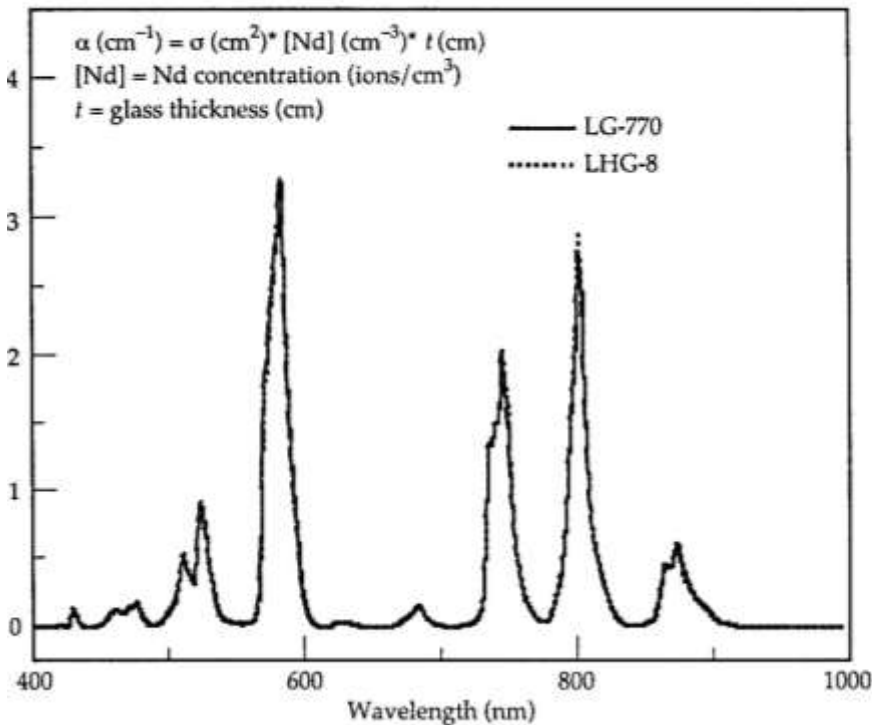
$$B_{21} = \frac{c}{h\nu g(\nu)} \sigma(\nu), \tag{1.49}$$

where $c = c_0/n_0$ is the speed of light in the medium. The energy density per unit frequency (ν) is expressed in terms of the lineshape factor $g(\nu)$, the energy $h\nu$, and the photon density φ (photons/cm³).

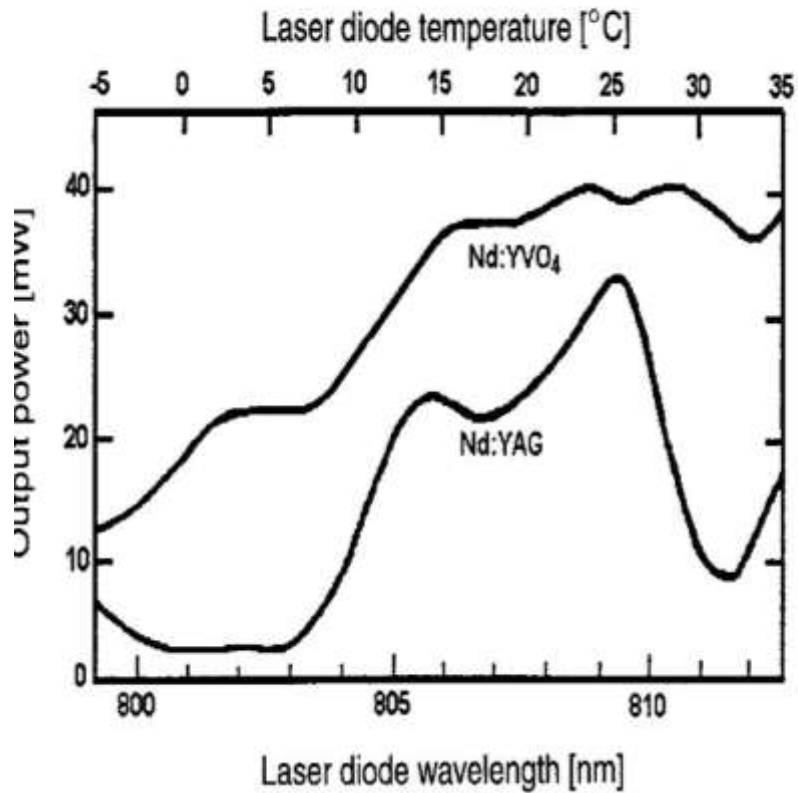
Transfer process		Multimode	Single mode
Diode slope efficiency	η_P	0.50	0.50
Transfer efficiency	η_t	0.95	0.95
Absorption efficiency	η_a	0.90	0.90
Stokes shift	η_S	0.76	0.76
Quantum efficiency	η_Q	0.95	0.95
Coupling efficiency	η_C	0.90	0.90
Beam overlap efficiency	η_B	0.90	0.38
Electrical slope efficiency	σ_S	0.25	0.10

Second, the emission lines of ions in glasses are inherently broader than in crystals. A wider line increases the laser threshold value of amplification. Nevertheless, this broadening has an advantage. A broader line offers the possibility of obtaining and amplifying shorter light pulses and, in addition, it permits the storage of larger amounts of energy in the amplifying medium for the same linear amplification coefficient. Thus, glass and crystalline lasers complement each other. For continuous or very high repetition-rate operation, crystalline materials provide higher gain and greater thermal conductivity. Glasses are more suitable for high-energy pulsed operation because of their large size, flexibility in their physical parameters, and the broadened fluorescent line.

Properties of Solid-State Laser Materials

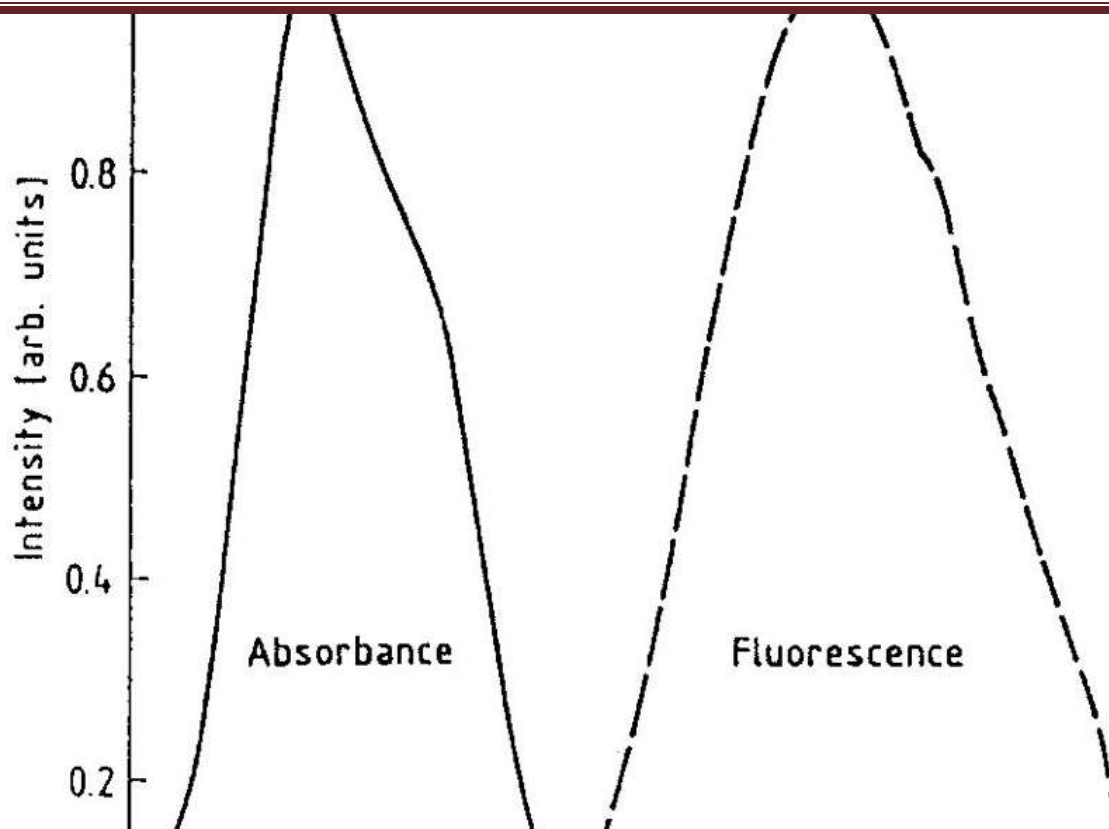


Solid-State Laser Materials



- Ti:Sapphire

Since laser action was first reported, the Ti : Al₂O₃ laser has been the subject of extensive investigations and today it is the most widely used tunable solid-state laser. The Ti : sapphire laser combines a broad tuning range of about 400 nm with a relatively large gain cross section that is half of Nd : YAG at the peak of its tuning range. The energy level structure of the Ti³⁺ ion is unique among transition-metal laser ions in that there are no *d* state energy levels above the upper laser level. The simple energy-level structure ($3d^1$ configuration) eliminates the possibility of excited-state absorption of the laser radiation, an effect which has limited the tuning range and reduced the efficiency of other transition-metal-doped lasers.



Conclusions

The current study on SIMULATE FINE STRUCTURES SOLID STATE LASERS USING OBJECT ORIENTED PROGRAMMING

the results shows that the thermal equilibrium lower energy states of ions or atoms are more heavily populated than higher energy states according to Boltzmann's statistics. In order for stimulated emission rather than absorption to occur, the population between two energy states has to be inverted, such that the higher energy level is more heavily populated compared to the lower level. Energy to achieve this population inversion is supplied by a pump source. In a three-level laser the ground state of the electronic transition is also the lower laser level. At thermal equilibrium the majority of ions are in this level. Thus, at least half of the ions at the ground level must be transferred to the upper laser level before laser action is possible.

Historically it was Wolfgang Pauli who postulated magnetic angular momentum in 1924 whereas Back and Goudsmith made the first detailed study of the bismuth hyperfine structure in 1927. Thus it was the hyperfine structure studies that triggered and opened up all altogether new vista into nuclear physics in an era of, what is now termed as Spectral Zoology [121]. Hyperfine structural studies have also been helpful in laser based isotope separation as well as definitions of fundamental quantities like time and their respective measurements. Emerging technologies like quantum informatics are also employing hyperfine states of trapped ions for their decoherence resistant operations [80]. Moreover in astrophysical investigations the abundance of the La II in cosmic objects, calculated on the basis of the spectral line analysis, gives the information about the nucleosynthesis of chemical elements. It is well known that the system of electronic levels is moderately affected by the crystalline lattice. Therefore, many features characteristic of the spectra of free atom and ion of lanthanide remain preserved for lanthanide ions implemented in crystals. It is one of the reasons for the wide interest in the application of the lanthanides with their unique hyperfine structures as active media in lasers or quantum memories and repeaters.

various research groups utilizing a multitude of techniques. Chapter 4 elaborates mainly on the various techniques usually employed for the investigation of the atomic hyperfine structure. Our employed technique i.e. laser induced fluorescence spectroscopy for hfs is described at length covering merits and demerits of the method. Different computer programs used for the data acquisition are described at length along with the procedure employed for analysis of the LIF recorded data hfs also been sketched in this chapter. Finally in Chapter 5, we give the detailed report on our results i.e. the characterization of known levels as well as the discovery of new levels along with the significant differences for the values of the hyperfine constants observed for other four level.

To summarize, in the present work FT spectra of Lanthanum was generated in the spectral range of 3800-8800 cm^{-1} . The FT data sets provided in digitalized form by a group in Riga (R. Ferber, A. Jarmola, M. Tamanis, Department of Physics, University of Latvia, Raina bulvaris, Riga). The same was converted in the graphical form at TU Craiova before starting the present experimental work. Salient features of FT spectra, such as high resolution (0.03 cm^{-1} for La), large spectral range coverage and accurate position of the hyperfine components proved to be quite helpful for measuring the center of gravity of most of the excitation lines very accurately. In our results described in Table 1, we have mostly taken the c.o.g. of an excited line from the FT simulation provided that the hf structure is well resolved in FT spectra, otherwise from the Fitter if the hf structure are not fully resolved or encountered with a blend situation. Moreover, it has served as an efficient tool not only for finding the new levels as well as for the investigation of new lines with known level which were not listed yet in commonly used NIST table. In the present study of more than 155 spectral lines of lanthanum, about half of the lines were new La lines, found on the basis of these highly resolved FT spectra. Furthermore the intensity of most of the new lines investigated was very low (>5) but the LIF signal recorded was sufficiently strong, which proved the LIF detection a good technique.

References

- [1] A. J. Schokker, Associate Professor, Civil and Environmental Engineering, The Pennsylvania State University. Personal Communication. Aug. 2004.
- [2] B. M. Luccioni, R. D. Ambrosini, and R. F. Danesi, "Analysis of Building Collapse Under Blast Loads," *Engineering Structures*, Vol. 26, 2004, pp. 63–71.
- [3] AUTODYN, "Interactive Non-Linear Dynamic Analysis Software, Version 4.2, User's Manual," Century Dynamics Inc., 2001.
- [4] G. Mazar, O. Igra, G. Ben-Dor, M. Mond, and H. Reichenbach, "Head-On Collision of Normal Waves with a Rubber-Supported Wall," *Philosophical Transactions: Physical Sciences and Engineering*, Vol. 338, No. 1650, 1992.
- [5] W. Bleakney, D. R. White, and W. C. Griffith, "Measurements of Diffraction of Shock Waves and Resulting Loading on Structures," *Journal of Applied Mechanics*, Vol. 17, Dec. 1950, pp. 439–445.
- [6] J. K. Wright, *Shock Tubes*, John Wiley & Sons Inc., 1961.
- [7] O. Igra, X. Wu, J. Falcovitz, T. Meguro, K. Takayama, and W. Heilig, "Experimental and Theoretical Study of Shock Wave Propagation Through Double-Bend Ducts," *Journal of Fluid Mechanics*, Vol. 437, 2001, pp. 255–282.
- [8] O. Igra, J. Falcovitz, H. Reichenbach, and W. Heilig, "Experimental and Numerical Study of the Interaction between a Planar Shock Wave and a Square Cavity," *Journal of Fluid Mechanics*, Vol. 313, 1996, pp. 105–130.
- [9] P. Neuwald, H. Klein, and H. Reichenbach, "Unsteady Flows Inside Structures - High Speed Visualization as a Tool for Numerical Modeling and Code Validation," *SPIE*, Vol. 2869, 1996, pp. 798–806.
- [10] H. Reichenbach and P. Neuwald, "Indoor Detonations - Visualization and Pressure Measurements in Small-Scale Models," *SPIE*, Vol. 4183, 2000, pp. 92–104.
- [11] D. C. Pack, "The Reflection and Transmission of Shock Waves I: The Reflection of a Detonation Wave at a Boundary," *Philosophical Magazine*, Vol. 2, No. 14, 1956, pp. 182–188. 122

- [12] D. C. Pack, "The Reflection and Transmission of Shock Waves II: The Effect of Shock Waves on an Elastic Target of Finite Thickness," *Philosophical Magazine*, Vol. 2, No. 14, 1956, pp. 182–188.
- [13] G. Taylor, "The Formation of a Blast Wave by a Very Intense Explosion. I. Theoretical Discussion," *Proceedings of the Royal Society of London. Series A*, Vol. 201, No. 1065, 1950, pp. 159–174.
- [14] G. Taylor, "The Formation of a Blast Wave by a Very Intense Explosion. II. The Atomic Explosion of 1945," *Proceedings of the Royal Society of London. Series A*, Vol. 201, No. 1065, 1950, pp. 175–186.
- [15] O. Igra, T. Elperin, and G. Ben-Dor, "Blast Waves in Dusty Gases," *Proceedings of the Royal Society of London. Series A*, Vol. 414, No. 1946, 1987, pp. 197–219.
- [16] J. Glimm, "Solutions in the Large for Nonlinear Hyperbolic Systems of Equations," *Communications on Pure and Applied Mathematics*, Vol. 18, 1965, pp. 697–715.
- [17] H. Miura and I. I. Glass, "On a Dusty-Gas Shock Tube," *Proceedings of the Royal Society of London. Series A*, Vol. 382, No. 1783, 1982, pp. 373–388.
- [18] P. Colella, "Glimm's Method for Gas Dynamics," *SIAM Journal on Scientific and Statistical Computing*, Vol. 3, No. 1, 1982, pp. 76–110.
- [19] W. G. Penney, Geoffrey Taylor, H. Jones, W. M. Evans, R. M. Davies, J. D. Owen, D. H. Edwards, D. E. Thomas, C. A. Adams, F. P. Bowden, A. R. Ubbelohde, J. S. Courtney-Pratt, S. Paterson, J. Taylor, and O. A. Gurton, "A Discussion on Detonation," *Proceedings of the Royal Society of London. Series A*, Vol. 204, No. 1076, 1950, pp. 1–33.
- [20] L. N. Long and J. B. Anderson, "The Simulation of Detonations using a Monte Carlo Method," in *22nd International Symposium on Rarefied Gas Dynamics*, Sydney, Australia, July 2000.
- [21] J. B. Anderson and L. N. Long, "Direct Monte Carlo Simulation of Chemical Reaction Systems: Prediction of Ultrafast Detonations," *Journal of Chemical Physics*, Vol. 118, No. 7, 2003, pp. 3102–3110.
- [22] P. O'Connor, L. N. Long, and J. B. Anderson, "Monte Carlo Simulations of Ultrafast Detonations in Mixtures," in *24th International Symposium on Rarefied Gas Dynamics*, Bari, Italy, 2004.
- [23] D. L. Chapman, *Philosophical Magazine*, Vol. 47, 1899.
- [24] E. Jouguet, "Mecanique des Explosifs," *Journal Mathematique*, Vol. 347, 1905.

M. J. Nye (Ed.), *The Cambridge History of Science: The Modern Physical and Mathematical Science*, Cambridge University Press (2003).

- [2] M. Jammer, *The Philosophy of Quantum Mechanics: The Interpretation of Quantum Mechanics in Historical Perspective*, John Wiley & Sons (1976).
- [3] Michelson, *Phil. Mag.* 31, 338 (1891).
- [4] C. Fabry and A. Perot, *Ann. Chim. et Phys.* 12, 459 (1897).
- [5] O. Lummer and E. Gehreke, *Ann. Phys.* 10, 457 (1903).
- [6] W. Pauli, *Naturwissenschaften* 12, 74 (1924).
- [7] E. Back and S. Goudsmit, *Z. Physik* 43, 321 (1927); 47, 74 (1928).
- [8] D. A. Jackson, *Proc. Roy. Soc. (London)* AX21, 432 (1928).
- [9] De Broglie, *Phil. Mag.* 47, 446 (1924)
- [10] E. Schrödinger, *Ann. Physik* 79, 361, 489, 734 (1926); 80, 437 (1926); 81, 109 (1926).
- [11] E. Fermi, *Z. Physik* 60, 320 (1930)
- [12] G. Breit, *Phys. Rev.* 35, 1447 (1930); 37, 51 (1931). [13] S. Goudsmit, *Phys. Rev.* 37, 663 (1931).
- [14] G. Breit, *Phys. Rev.* 38, 463 (1931).

- [15] H. B. G. Casimir, On the interaction between Atomic Nuclei and Electrons (Teyler's Tweede Genootschap, Haarlem, 1936; W. H. Freeman, San Francisco, (1963)
- [16] H. B. G. Casimir and G. Karrman, *Physica* 9, 494 (1942).
- [17] H. Schuler and J. Keyston, *Naturwissenschaften* 19, 320 (1931).
- [18] H. Kopfermann, *Naturwissenschaften* 19, 400 (1931).
- [19] D. J. Hughes, C. Eckart, *Phys. Rev.* 36, 694 (1930).
- [20] W. Pauli and R. E. Peierls *Phys. Z.* 32, 670 (1931).
- [21] J. Rosenthal and G. Breit, *Phys. Rev.* 41, 459 (1932).
- [22] D. A. Jackson and H. Kuhn *Proc. Roy. Soc. A* 148, 335 (1935).
- [23] R. Minkowski, *Z Phys.* 95, 274 (1935).
- [24] G. Racah, *Phys. Rev.* 62, 438 (1942).
- [25] G. Racah, *Phys. Rev.* 63, 367 (1943).
- [26] G. Racah, *Phys. Rev.* 76, 1352 (1949).
- [27] R. E. Trees, *Phys. Rev.* 92, 308 (1953).
- [28] C. Schwartz, *Phys. Rev.* 97, 380 (1955).
- [29] P. G. H. Sandars and J. Beck, *Proc. Roy. Soc. (London)* A289, 97 (1955).
- [30] I. Rabi, S. M. Uman, P. Kusch, and J. R. Zacharias, *Phys. Rev.* 55, 526 (1939).
- [31] N. F. Ramsay, *Molecular Beams* (Oxford University Press, London, (1956).
- [32] J. Brossel and A. Kastler *Compt. Rend* 229, 1213 (1949). R. A. Bernheim, *Optical pumping: An Introduction* (W. A. Benjamin, Inc., New York, 1965). H. R. Schossberg and A. Javan, *Phys. Rev. Lett.* 17, 1242 (1966). /
- [33] J. R. Zacharias, *Phys. Rev.* 61, 270 (1942).

Research Methodology

The method was implemented in Simulate Fine Structures Solid State Lasers Using Object Oriented Programming as a plug-in module for AlphaCAM (Licom Ltd) computer-aided design software. The module has a VBA interface for parameter input with a C/C++ DLL mathematical engine. The results were visualized by the native AlphaCAM API. Any predictive simulation based on a phenomenological approach is only useful if the model parameters are known a priori or can be derived in a way much easier than actual trial ablation of the complete structures. The accuracy of the parameter values has to be adequate for quantitative modeling. Ideally parameters of the models should be calibrated from ablation of relatively simple shapes like a series of single shot craters, for instance. For all our simulations fitting of the single crater profile was used for calibration of the AC parameters. To find the best fit each model was tried in turn. An initial tool path for the intended structure was generated by standard tools of AlphaCAM. The tool path was converted into a laser shot map by setting the feed rate of the scanner and the laser repetition rate. The resulting simulated surface was compared with the intended design. The tool path, feed rate and repetition rate were modified until the simulated shape replicated the design.